OBSERVATION OF EARTHQUAKE RESPONSE OF GROUND WITH HORIZONTAL AND VERTICAL SEISMOMETER ARRAYS (2ND REPORT)

Hajime Tsuchida[I], Setsuo Noda[II], Susumu Iai[III], and Eiichi Kurata[III]

SUMMARY

Seismic wave propagation in the surface layer was studied with ground motion records of three earthquakes observed by a vertical two dimensional accelerometer array. Frequency response functions were calculated for many combinations of two accelerometer points for this study. The results show that seismic wave propagates through almost the same path in the surface layer regardless of locations or characteristics of earthquakes. The results deny a conception that seismic wave propagates straightly without deformation along the ground surface but they are not contradictory to the multiple reflection of shear waves in the vertical direction in the surface layer.

INTRODUCTION

Many researchers and engineers are interested in knowing how the seismic waves propagate in the surface layer on the base rock and what are the input seismic waves to the surface layer. The authors have established two dimensional seismometer array, in other words, a seismometer system with accelerometers deployed in a vertical plane in the ground. This paper presents analysis of the records of the array from viewpoint of seismic wave propagation in the surface layer.

The array and some of records from the array have already been presented in a paper 1), which will be called the first report hereinafter. In the first report, the records were analyzed with emphasis on relative motions among the accelerometer points on the ground surface.

ARRAY

The array has been installed in a part of the Tokyo International Airport. It consists of six ground surface accelerometers and four downhole accelerometers. Two of the four downhole accelerometers have been installed just below the ground surface together with the ground surface accelerometers. They are intended to confirm the ground surface accelerometer and the downhole accelerometer present indetical ground acceleration records.

The ground surface accelerometers are located at an equal spacing of 500 meters along a straight line of a total length 2500 meters. Each accelerometer consists of two horizontal components parallel and prependicular to the observation line. The downhole accelerometers are three component ones; two components are horizontal ones parallel and perpendicular to the

I Chief, Earthquake Resistant Structures Laboratory, Structures Division, Port and Harbour Research Institute, Ministry of Transport.
II Chief, Earthquake Disaster Prevention Laboratory, Structures Division, Port and Harbour Research Institute, Ministry of Transport.
III Member, Earthquake Resistant Structures Laboratory, Structures Division, Port and Harbour Research Institute, Ministry of Transport.

observation line, and one component is vertical one. Fig. 1, shows the deployment of the accelerometers in the vertical section of the ground at the array site.

Fig. 1 also shows the subsoil conditions at the site. The lower downhole accelerometers were originally intended to be settled in real base rock. However, the rock formation is so deep here that the downhole accelerometers were installed in a stiff diluvial deposit. This deposit will be called a base layer in this paper.

The points of accelerometer locations at the ground surface will be designated as the alphabetical letters indicated in Fig. 1. The downhole accelerometer locations in the base layer will be designated as A67 and E50 as idicated also in Fig. 1. In some of the figures they will be indicated as A(base) and E(base).

RECORDS

Records of three earthquake designated as TIA-3, TIA-6, and TIA-9 were selected for the analysis. Earthquake data are given in Table 1. Averages of maximum horizontal component accelerations at the ground surface are 15.3, 9.6, and 33.9 gals for TIA-3, TIA-6, and TIA-9, respectively. Locations of epicenters of the earthquakes are shown in Fig. 2, in which the direction of the observation line is indicated as D.H.A. Fig. 3 shows an example of the records of the components parallel to the observation line.

PROCEDURE FOR ANALYSIS

Frequency response functions (FRF) were calculated to study correlation of earthquake ground motions between two points of various combinations. Recorded ground motion at one point was regarded as input of the FRF and that at the other point as output. For calculating FRF, a smoothing window was used, of which equivalent window width was 0.2 Hz.

RESULTS OF THE ANALYSIS

Calculated FRF will be presented in this section. For making comparison of FRF for different components and different earthquakes easier, FRF of the three earthquakes are plotted in one graph, besides FRF of two horizontal components are plotted together. As the result, six FRF of the horizontal ground motions are presented together in one graph, and three FRF of the vertical ground motions are presented together.

FRF in horizontal direction at surface

Amplifications of FRF between the points A and B, B and C, and A and F are shown in Figs. 4 through 6. It will be noticed that the amplifications change as the frequency changes. It will aslo be noticed that the six FRF of each combination of the points show similar shapes.

FRF in vertical direction

Amplification of FRF between the points A and A67 and between the points E and E50 are shown in Figs. 8 through 11. Figs. 8 and 9 show FRF of the

horizontal ground motions. It is clearly seen that there is similarity among FRF of the horizontal ground motions, especially in their peak frequencies. FRF of the vertical ground motions of three earthquakes have similar tendencies, while there is no peak as sharp as that seen in FRF of the horizontal ground motions.

FRF in horizontal direction in base layer

FRF between the points A67 and E50 are shown in Figs. 12 and 13. Amplifications of FRF of the horizontal ground motions are not unity nor constant. However, there is similarity among the six amplification curves in the frequency range lower than about 6 Hz.

CONSIDERATIONS

Similarity of seismic wave propagation path regardless of earthquakes

The results of the analysis show that FRF of any combinations of two points are similar to each other regardless of locations or characteristics of three earthquakes. This similarity indicates that seismic wave propagates through almost the same path in the surface layer at any earthquakes. It also indicates that input ground motions to the various points on the boundary of the surface layer are correlated each other at any earthquakes.

Deformation of seismic wave during propagation

If the seismic waves propagate straightly in the ground and no deformation of waves takes place during the propagation, amplification of FRF is unity regardless of the frequency, and phase of FRF varies in proportion to the frequency. The analysis shows that the amplifications of FRF in the horizontal direction at the ground surface change as the frequency changes. This is denying a conception that the seismic waves propagate straightly in a constant amplitude along the ground surface. The phases of FRF in the horizontal direction denies this conception, too.

A seismic propagation model

There may be many possible seismic wave propagation models which are not contradictory to the results of the analysis presented previously. Concerning to the result of the horizontal motions, one of the possible and simple models is the multiple reflection of shear waves in the vertical direction at each site.

FRF of the sites A and E based on the multiple reflection theory are calculated with the data of shear wave velocities measured at each site. The shear wave velocities were measured using artificially generated shear waves propagating vertically into the ground. The results are shown in Fig. 14. The peak frequencies of FRF from the earthquake observation and those from the shear wave velocities agreed very well, especially in regard to the lower three natural frequencies. This agreement is one of the supports for the conception that the seismic waves propagate vertically in the surface layer, at least, in a layer of similar scale to that of the observation site of the array. This model can also explain the result that FRF in the horizontal direction are not unity both at the ground surface and in the base layer.

Assumption of common incident wave

When seismic waves are considered to propagate vertically in the surface layer, it is often assumed that incident waves at the adjacent points located within the scale of this array is common to each other. For studying this assumption, incident waves were calculated with the theory of multiple reflection and compared in form of FRF between the points A67 and E50. The results are shown in Fig. 15. This figure indicates that the calculated incident waves are not identical but there are correlation of some extent regardless of the earthquakes and the components in the horizontal directions.

Acceleration time histories of the incident waves at the two points are compared in Fig. 16. Displacement time histories were calculated from the acceleration time histories and shown in Fig. 17. As it is seen there, agreement in the low frequency components is rather good. The same thing can be read from Fig. 15. When only low frequency components of earthquake ground motions are of importance, the assumption of the common incident wave seems to be one of the applicable approaches.

The difference in the high frequency components in the incident waves at the points A67 and E50 may be improved by adjusting the shear wave velocities and the thickness of layers. However, the authors are not sure whether the difference is caused by the conception of vertical propagation of seismic waves or by the parameter selection. This will be studied further in the future.

CONCLUSIONS

The records of three of the earthquakes from the two dimensional accelerometer array were analyzed for studying the seismic wave propagation in the surface layer.

The results show that seismic wave propagates through almost the same path in the surface layer regardless of locations or characteristics of earthquakes and that input ground motions to the various points on the boundary of the surface layer are correlated each other at any earthquakes.

The results deny a conception that seismic wave propagates straightly without deformation along the ground surface.

The frequency response functions calculated with shear wave velocities measured at the site based on the theory of multiple reflection agreed very well with the frequency response functions calculated from the earthquake records.

REFERENCE

1) Tsuchida, H., Kurata, E., and Hayashi, S. 1977: Observation of earthquake response of ground with horizontal and vertical seismometer arrays, Proceedings of the 6th World Conference on Earthquake Engineering, Vol. 1, pp. 509-515.

Record Designation	TIA-3	TIA-6	TIA-9
Date	May 9, 1974	July 8, 1974	August 4, 1974
Time	08:33	14:15	03:17
Latitude of the epicenter	33.6° N	- 36.4° N	36.0° N
Longitude of the epicenter	138.8° E	141.2° E	139.9° E
Azimuth to the Epicenter*	S 40° W	N 53° E	N 14° E
Epicentral Distance	140 km	161 km	54 km
Depth of the Hypocenter	10 km	40 km	50 km
Magnitude	6.9	6.3	5.8

* Direction of observation line of the array is N 27° W and point F is at north end.

Table 1 Earthquake Data

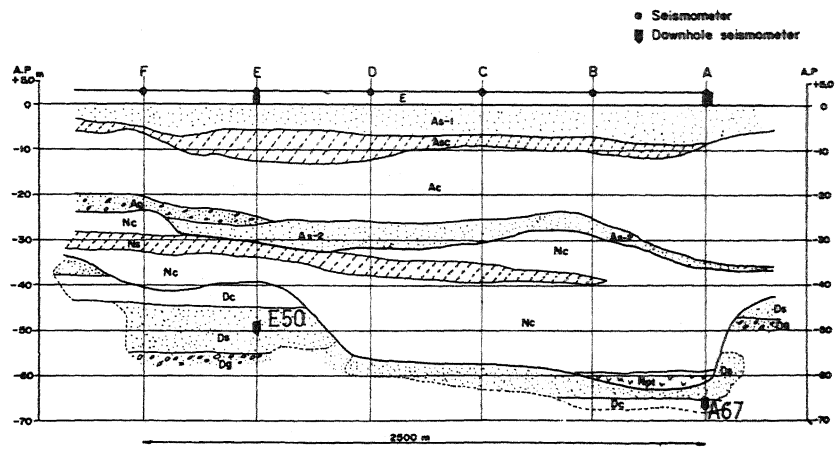

Key (Fill) E : Fill, (Alluvial deposit) A_{s-1} : Sand, A_{sc} : Silty sand, A_c : Silty clay, A_{s-2} : Sand, A_g : Sandy gravel, (Diluvial deposit) N_c : Silty clay, N_s : Silty sand, N_{pt} : Peat, D_s : Sand, D_g : Sandy gravel, D_c : Silt.

Fig. 1 The Deployment of the Accelerometers in a Vertical Section

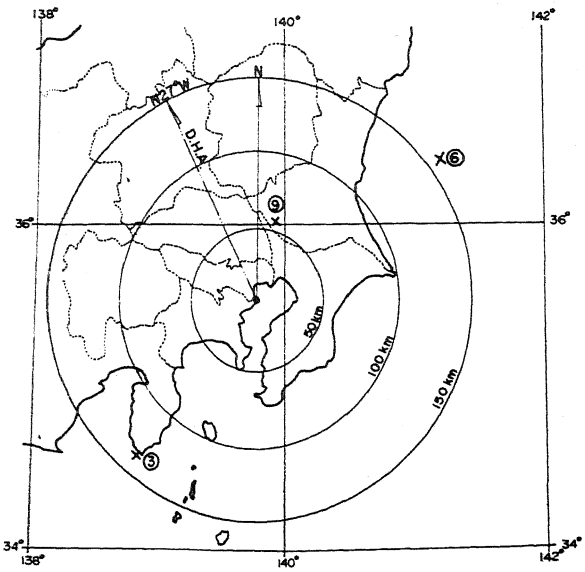

Fig. 2 Locations of Epicenters of Earthquakes TIA-3, 6, and 9

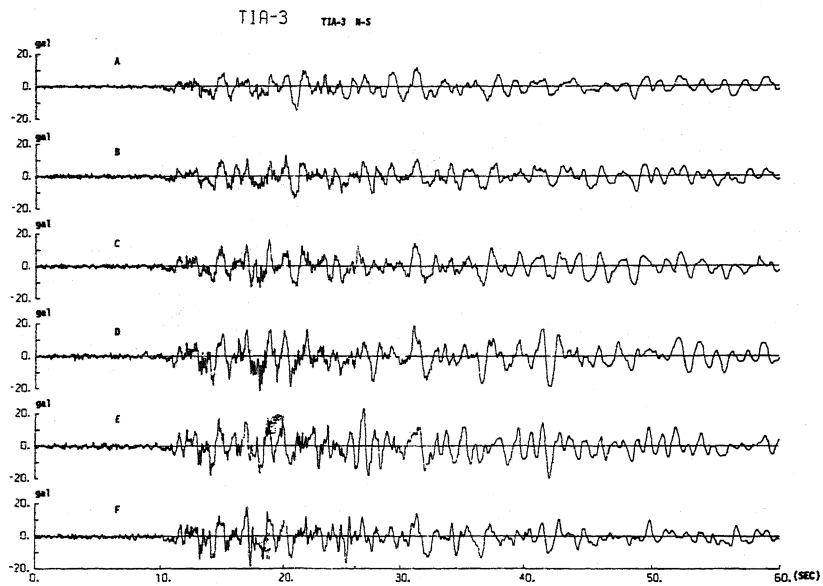

Fig. 3 An Example of the Records of the Components Parallel to the Observation Line

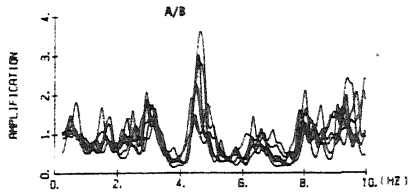

Fig. 4 FRF (amp.) A/B

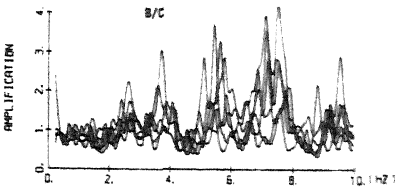

Fig. 5 FRF (amp.) B/C

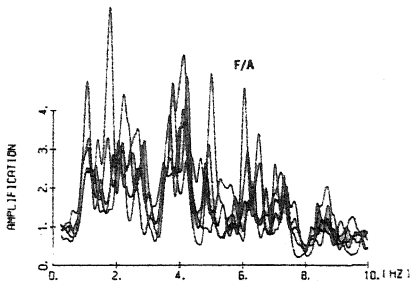

Fig. 6 FRF (amp.) F/A

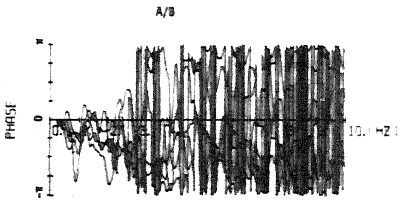

Fig. 7 FRF (phase) A/B

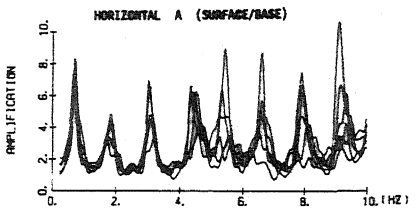

Fig.8 FRF (amp.) at A (Surface/Base) Horizontal

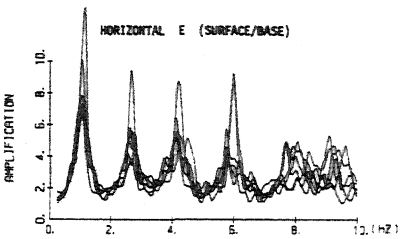

Fig.9 FRF (amp.) at E (Surface/Base) Horizontal

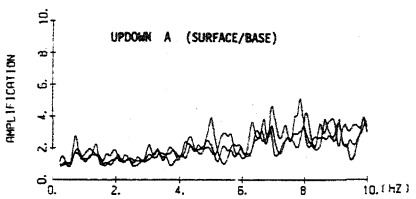

Fig. 10 FRF (amp.) at A (Surface/Base) U - D

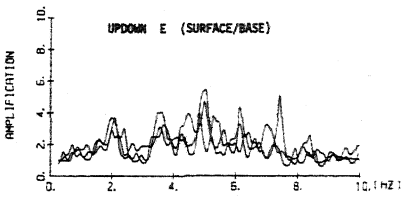

Fig. 11 FRF (amp,) at E (Surface/Base) U - D

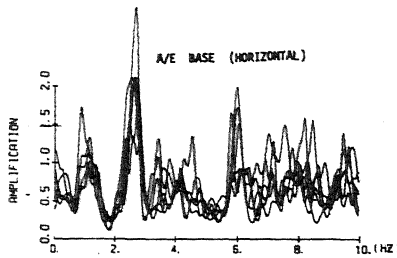

Fig.12 FRF(amp.) A67/E50 (Horizontal)

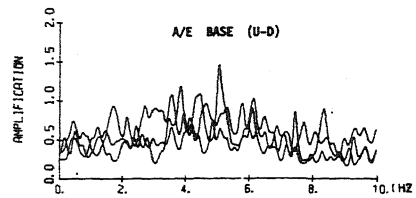

Fig.13 FRF (amp.) A67/E50 (UD)

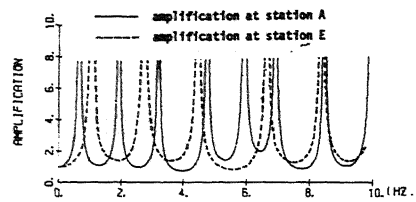

Fig.14 FRF (amp.) of Multiple Reflection Model

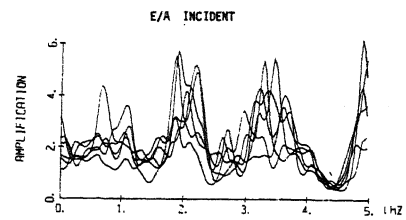

Fig.15 FRF (amp.) E/A (Calculated Incident Waves)

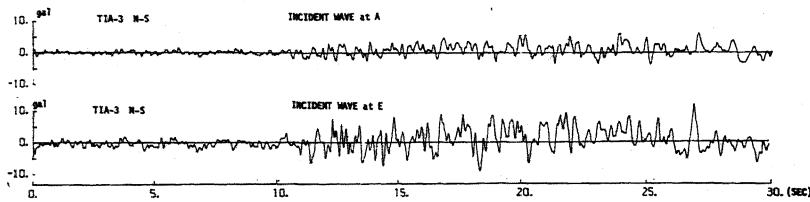

Fig. 16 Incident Waves at A and E (Acceleration)

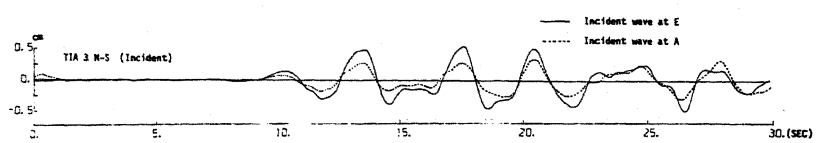

Fig. 17 Incident Waves at A and E (Displacement)